

MetaTime v36.5: Non-Markovian Cosmological Dynamics from Future-Latency Dark-Sector Exchange

Minimal Bridge from Ontology to Effective Closure and a New Expansion-Growth Hysteresis Observable

Darío Peyrú¹

¹*Independent Researcher, Pilar, Buenos Aires, Argentina*

(Dated: April 17, 2026)

MetaTime v36.2 established a solver-ready non-Markovian interacting-dark-sector model with a latent memory variable $m(x)$, $x \equiv \ln a$, an open-EFT motivation for a retarded kernel, a physically anchored memory width Δ , and controlled background and perturbation equations. MetaTime v36.3 preserved that machinery while reinterpreting the latent density as future latency, and v36.4 added a minimal bridge from that ontology to the effective closure $Q = 3H\beta_{\text{eff}}(x)\rho_F$. The present v36.5 step introduces a sharper observational discriminant. We show that once the latent sector is read as a memory-bearing reservoir of future latency, the model generically predicts a nonzero hysteresis area in the expansion-growth plane: two proxy histories with the same present value can yield slightly different $f\sigma_8$ responses at matched H/H_0 . We define this matched-expansion diagnostic by $\Delta_{f\sigma_8|H}(H)$ and the associated area functional $\mathcal{A}_{\text{hyst}}$, which vanishes in the Markovian limit and survives for finite Δ . The background equations, perturbative closure, PPF bridge, certification tests, and inherited benchmark figures are preserved. What is new is that the path dependence already present in the latent state is promoted to a directly plotable observable in the $(H/H_0, f\sigma_8)$ plane. The resulting framework remains conservative at the level of implementation while becoming more falsifiable: it no longer predicts only delayed-response dark-sector exchange, but a concrete expansion-growth hysteresis signature of future-latency cosmology. We also include a lightweight pilot comparison against public late-time $H(z)$ and $f\sigma_8$ compilations. In that preliminary test the model remains competitive with Λ CDM in raw χ^2 , while the preferred region lies close to the Markovian limit.

I. INTRODUCTION

Interacting dark-energy and dark-sector-exchange models are typically judged by two criteria: whether the background closure preserves overall conservation and whether the perturbation sector remains numerically controlled on large scales. MetaTime v36.0 addressed these requirements with a conservative exchange law and a parameterized post-Friedmann (PPF) bridge. MetaTime v36.1 replaced an instantaneous schedule by a history-dependent response, and MetaTime v36.2 consolidated that upgrade by supplying an open-EFT motivation for the retarded kernel, a physical anchoring for the memory width Δ , and a controlled perturbative implementation [1, 2].

MetaTime v36.3 left the technical backbone intact but sharpened the interpretation of the latent sector: the variable ρ_L was no longer read merely as an abstract hidden component, but as the gravitationally active reservoir of compressed future states. The present v36.5 step goes one notch further. Its goal is not to modify the operational equations, but to make explicit why the v36.2 closure is the natural minimal effective form once the latent sector is interpreted as future latency. A separate conceptual note developed this identification in stand-alone form [3]; here it is folded back into the cosmological framework.

The working identification is

$$\rho_L \equiv \rho_F, \quad (1)$$

where ρ_F denotes the density of physically admissible but not-yet-executed future states. The claim is not that already-realized future events act backward in time. The claim is rather that a finite-bandwidth cosmology may contain a latent stock of physically weighted future-state capacity, and that this stock may gravitate while remaining electromagnetically dark until execution.

Under this reading, the conservative continuity system

$$\dot{\rho}_L + 3H\rho_L = +Q, \quad (2)$$

$$\dot{\rho}_I + 3H(1 + w_I)\rho_I = -Q, \quad (3)$$

retains its form, but the exchange term acquires a more specific meaning. Rather than a generic dark-sector transfer, it becomes an effective future-to-present execution or decompression flow. The main task of v36.4 is to show why the same operational closure used previously,

$$Q = 3H\beta_{\text{eff}}(x)\rho_L, \quad (4)$$

is the minimal effective realization of that idea.

II. OPEN-EFT ORIGIN OF THE RETARDED KERNEL

The open-EFT logic of v36.2 remains unchanged. Unresolved processing degrees of freedom may be integrated out through Schwinger–Keldysh/Feynman–Vernon methods, leaving a retarded non-local influence

on the retained dark-sector variables. Schematically,

$$S_{\text{eff}} = S_{\text{loc}} + \int dx dx' \mathcal{O}(x) K(x, x') \mathcal{O}(x') + \dots, \quad (5)$$

where \mathcal{O} denotes the retained operator and K is a retarded kernel.

For slowly varying histories, the minimal one-pole realization is the normalized exponential kernel

$$K(\Delta x) = \frac{1}{\Delta} e^{-\Delta x / \Delta} \Theta(\Delta x), \quad \Delta x \equiv x - x'. \quad (6)$$

This choice is causal, positive, and reducible to a first-order auxiliary equation. It should be interpreted as the minimal operational embedding of retardation rather than as a claim that the exact microscopic kernel is strictly exponential.

The latent memory variable is then defined by

$$m(x) = \int_{-\infty}^x dx' K(x - x') \hat{b}_{\Pi}(x'), \quad (7)$$

with effective coupling

$$\beta_{\text{eff}}(x) = \beta_0 + \beta_1 m(x), \quad (8)$$

and interaction law

$$Q = 3H\beta_{\text{eff}}(x)\rho_L. \quad (9)$$

The corresponding auxiliary evolution equation is

$$m'(x) = \frac{\hat{b}_{\Pi}(x) - m(x)}{\Delta}, \quad (10)$$

where prime denotes d/dx with $x = \ln a$. The strict regression channel is immediate: as $\Delta \rightarrow 0$, one recovers $m \rightarrow \hat{b}_{\Pi}$ and therefore the Markovian v36.0 closure.

III. PHYSICAL ANCHORING OF THE MEMORY WIDTH

The dimensionless memory width Δ is best interpreted as a relaxation scale measured in e-fold time. If the unresolved processing sector is characterized by a relaxation time τ_{Π} in cosmic time, then locally

$$\Delta(a) \sim H(a)\tau_{\Pi}(a). \quad (11)$$

Around a pivot epoch where the interaction is active one may write

$$\Delta_* \simeq H_* \tau_{\Pi,*} \sim \frac{H_*}{m_{\Pi,*}}, \quad (12)$$

if the sector is associated with an effective mass scale $m_{\Pi,*} \sim \tau_{\Pi,*}^{-1}$.

This relation provides the same three phenomenological regimes emphasized in v36.2: a Markovian regime $\Delta \ll 1$, an observable hysteresis regime $\Delta \sim \mathcal{O}(0.1-1)$, and a frozen-memory regime $\Delta \gg 1$. In v36.4 the same timescale is re-read as the relaxation time of locally available future latency.

IV. FUTURE-LATENCY INTERPRETATION OF THE LATENT SECTOR

The interpretive core is that the latent sector may be understood as the gravitationally active reservoir of compressed future states,

$$\rho_L \equiv \rho_F, \quad (13)$$

with ρ_F denoting future latency. One may encode that idea at a coarse-grained level by introducing the admissible-future set

$$\mathcal{F}(x, t) = \left\{ \begin{array}{l} \text{microstates physically admissible but} \\ \text{not yet executed at } (x, t) \end{array} \right\}, \quad (14)$$

and a corresponding density

$$\rho_F(x, t) = \epsilon_* \mu[\mathcal{F}(x, t)], \quad (15)$$

where μ is a coarse-grained measure on future-state capacity and ϵ_* is an effective energy weight per admissible latent unit. Equation (15) is not meant as a UV-complete definition, but as a compact statement that future latency is treated as physically weighted rather than merely symbolic.

Under this reading, the latent component can gravitate without having entered luminous or dissipative baryonic channels. The same delayed-response structure that appeared in v36.2 now acquires a more specific meaning: the memory variable $m(x)$ parameterizes the retarded persistence of locally available future information. Two histories with identical present proxy value but different past support may therefore yield different present $m(0)$ and hence different present effective couplings. The hysteresis built into the mathematics is reinterpreted as path dependence in the available future itself.

V. FROM FUTURE-LATENCY ONTOLOGY TO THE EFFECTIVE CLOSURE

The v36.4 bridge is preserved here, and the new v36.5 contribution is observational rather than structural: it makes explicit why the effective closure of v36.2 is the natural minimal realization of the future-latency picture.

At the coarsest level, any finite-rate execution process should satisfy a stock-flow principle: the magnitude of the exchange between latent and executed sectors must scale with the available latent stock. In an FRW background, the natural cosmological rate scale is H . Dimensional analysis therefore suggests a leading-order exchange magnitude of the form

$$|Q| \propto H\rho_F. \quad (16)$$

Introducing a dimensionless efficiency factor $\beta_{\text{eff}}(x)$ gives the minimal closure

$$Q \equiv 3H\beta_{\text{eff}}(x)\rho_F. \quad (17)$$

This is precisely the operational structure already used in v36.2. Its role here is not newly invented; it is newly justified.

Why should $\beta_{\text{eff}}(x)$ be history-dependent? Because the latent stock is not assumed to be instantaneously accessible. If the local availability of future states is mediated by an unresolved processing sector, then the effective execution efficiency should respond with delay to the proxy history controlling that sector. The minimal one-pole realization is therefore

$$\beta_{\text{eff}}(x) = \beta_0 + \beta_1 m(x), \quad m'(x) = \frac{\hat{b}_\Pi(x) - m(x)}{\Delta}. \quad (18)$$

The Markovian limit $\Delta \rightarrow 0$ corresponds to instantaneous scheduling; finite Δ encodes execution lag in the local availability of future latency.

The continuity equations may then be read as a balance law between future latency and executed cosmological structure,

$$\rho'_F + 3\rho_F = +3\beta_{\text{eff}}\rho_F, \quad (19)$$

$$\rho'_I + 3(1 + w_I)\rho_I = -3\beta_{\text{eff}}\rho_F, \quad (20)$$

with the sign convention inherited unchanged from v36.2. The important point is not the sign convention by itself, but the closure logic: once one accepts a finite-bandwidth stock of future latency, a transfer law proportional to $H\rho_F$ with a delayed dimensionless efficiency factor is the minimal effective choice compatible with conservation, FRW scaling, and regression to the local limit.

This is still not a unique UV derivation. Other non-linear or multi-pole closures could exist. But v36.4 clarifies that the v36.2 law is not an arbitrary ansatz: it is the leading-order effective closure naturally suggested by future-latency ontology plus finite-rate temporal processing.

VI. CONSERVATIVE EFT STATUS

The Einstein-frame consistency template remains deliberately modest. A broad class of effective actions of the form

$$S_{\text{eff}} = \int d^4x \sqrt{-g} \left[\frac{M_{\text{Pl}}^2}{2} R - \frac{1}{2} (\partial\phi)^2 - V(\phi) - \frac{1}{4} f_D(\phi) F_D^{\mu\nu} F_{\mu\nu}^D + \mathcal{L}_{\text{SM}} \right] + S_L + S_I + S_\Pi^{\text{open}}, \quad (21)$$

may, after integrating out unresolved degrees of freedom in S_Π^{open} , generate retarded contributions to the effective dark-sector coupling. The solver-facing closure used here is therefore consistent with a wide class of non-local Einstein-frame EFTs. It is best understood as a consistency template rather than a unique microscopic derivation. In v36.4, the same template is re-read as an EFT support structure for future-latency cosmology.

VII. LINEAR PERTURBATIONS AND CONTROLLED CLOSURE

The perturbative structure is inherited directly from v36.2. Working in synchronous gauge and choosing momentum transfer parallel to the cold component, the interacting latent sector obeys

$$\delta'_L = - \left(\theta_L + \frac{h'}{2} \right) + \frac{aQ}{\rho_L} \left(\frac{\delta Q}{Q} - \delta_L \right), \quad (22)$$

$$\theta'_L = -\mathcal{H}\theta_L, \quad (23)$$

while the executed negative-pressure sector obeys

$$\delta'_I = -(1 + w_I) \left(\theta_I + \frac{h'}{2} \right) - 3\mathcal{H}(\hat{c}_{s,I}^2 - w_I)\delta_I \quad (24)$$

$$- \frac{aQ}{\rho_I} \left(\frac{\delta Q}{Q} - \delta_I \right), \quad (25)$$

$$\theta'_I = -\mathcal{H}(1 - 3\hat{c}_{s,I}^2)\theta_I + \frac{\hat{c}_{s,I}^2}{1 + w_I} k^2 \delta_I - \frac{aQ}{\rho_I} (\theta_I - \theta_L). \quad (26)$$

The memory perturbation satisfies

$$\delta m' = \frac{\delta \hat{b}_\Pi - \delta m}{\Delta}, \quad \delta \beta_{\text{eff}} = \beta_1 \delta m. \quad (27)$$

The minimal implementation sets $\delta \hat{b}_\Pi = 0$, yielding $\delta m' = -\delta m/\Delta$, while an extended closure may be parameterized as $\delta \hat{b}_\Pi = b_\Pi \delta_L$. As in v36.2, the minimal approximation is controlled whenever $|\beta_1 b_\Pi| \ll 1$ over the observationally relevant regime.

The PPF bridge is also preserved,

$$k^2 \Phi = 4\pi G_N a^2 \sum_i \rho_i \Delta_i - k^2 \Gamma, \quad (28)$$

with

$$(1 + c_\Gamma^2 k_H^2)(\Gamma' + \mathcal{H}\Gamma) + c_\Gamma^2 k^2 \Gamma = S_\Gamma, \quad (29)$$

so that temporal non-locality enters through $\beta_{\text{eff}}(x)$ and $\delta \beta_{\text{eff}}$ while the quasi-static limit remains under control.

VIII. OBSERVABLE DISCRIMINANTS

The practical observational logic remains anchored in v36.2 [2], but v36.5 adds one sharper summary statistic. Increasing Δ delays the response of m to changes in the proxy history, thereby smoothing and phase-shifting the effective coupling relative to the Markovian baseline. The cleanest late-time discriminants remain: background deformations in $H(z)$, phase-shifted growth signatures in $f\sigma_8(z)$, and path dependence in large-scale potential evolution and integrated late-time CMB sensitivity.

The future-latency interpretation adds a sharper language for these signals, and v36.5 goes one step further

by promoting that language into a dedicated observable. If ρ_L is read as future latency, then hysteresis in observables at fixed present proxy value is naturally described as dependence on the prior history of locally available future states. The same data products remain relevant; what changes is the physical interpretation of why history matters.

A. Illustrative observable benchmarks

Because the operational equations of v36.4 are unchanged relative to v36.2, the same lightweight benchmark plots remain informative here. Figure 1 reproduces the exact background benchmark, the quasi-GR growth proxy, and the memory-smoothed effective coupling used in v36.2. Figure 2 reproduces the operational hysteresis benchmark showing how two proxy histories with the same present value but different past support generate distinct present effective couplings whenever $\Delta > 0$.

IX. A NEW OBSERVABLE: EXPANSION-GROWTH HYSTERESIS

The key observational upgrade of v36.5 is to turn path dependence of the latent state into a directly plotable late-time diagnostic. In a Markovian cosmology, the growth response is effectively a single-valued functional of the instantaneous expansion history. In the present framework, that degeneracy is broken: two histories with the same present proxy value and nearly overlapping late-time expansion histories can still yield slightly different growth responses because the execution efficiency carries memory through $m(x)$.

To formalize this point, consider two admissible proxy histories A and B satisfying

$$\hat{b}_{\Pi}^{(A)}(0) = \hat{b}_{\Pi}^{(B)}(0), \quad (30)$$

but differing in their past support. Their corresponding background and growth solutions generate two parametric curves,

$$\left(H^{(A)}(z), f\sigma_8^{(A)}(z) \right), \quad \left(H^{(B)}(z), f\sigma_8^{(B)}(z) \right), \quad (31)$$

in the expansion-growth plane. Matching the curves at equal H/H_0 defines the residual

$$\Delta_{f\sigma_8|H}(H) \equiv f\sigma_8^{(A)}(H) - f\sigma_8^{(B)}(H), \quad (32)$$

and the associated hysteresis area functional

$$\mathcal{A}_{\text{hyst}} \equiv \int_{H_{\min}}^{H_{\max}} |\Delta_{f\sigma_8|H}(H)| dH. \quad (33)$$

By construction,

$$\mathcal{A}_{\text{hyst}} \rightarrow 0 \quad \text{as} \quad \Delta \rightarrow 0, \quad (34)$$

or whenever the two histories collapse to the same latent-state evolution. For finite Δ , however, the memory-bearing future-latency sector generically yields $\mathcal{A}_{\text{hyst}} \neq 0$.

This quantity is not meant to replace a full likelihood analysis. It is a compact way to isolate the genuinely non-Markovian content of the model. Smooth deformations of $H(z)$ or of $f\sigma_8(z)$ individually can often be mimicked by other interacting-dark-sector prescriptions. A finite area in the $(H/H_0, f\sigma_8)$ plane is harder to mimic because it encodes path dependence at matched expansion rate. In the present framework, the physical interpretation is direct: the same instantaneous expansion can coexist with slightly different growth if the locally available future latency has a different prior history.

To visualize the effect, Fig. 3 shows a toy benchmark built from two proxy histories with equal present value but different past support. The left panel displays the constructed histories, the middle panel shows the corresponding growth responses, and the right panel displays the resulting finite band in the expansion-growth plane. The benchmark is intentionally lightweight and inherits the quasi-GR growth logic already used in v36.2, but it makes the new diagnostic explicit. What v36.5 adds to the earlier versions is therefore not a new kernel or a new perturbation equation, but a new observable summary of the same memory physics.

X. PILOT COMPARISON WITH REAL LATE-TIME DATA

To place the new hysteresis-oriented closure against currently available late-time observations, we include a lightweight pilot comparison using public compilations of $H(z)$ and $f\sigma_8(z)$. The exercise is intentionally modest. It uses diagonal observational errors only, no BAO, CMB, or supernova likelihoods, and it retains the quasi-GR growth proxy already used for the benchmark plots. The purpose is not to claim a precision constraint, but to test whether the future-latency closure is immediately disfavored or remains phenomenologically competitive.

We use 31 cosmic-chronometer points covering $0.07 \leq z \leq 1.965$ and 26 growth-rate points covering $0.013 \leq z \leq 1.944$. The pilot setup fixes $\Omega_{b0} = 0.05$, $\Omega_{r0} = 9 \times 10^{-5}$, $w_I = -1$, and $\beta_0 = 0$, while keeping the same smoothed proxy history used throughout the benchmark analysis. For the future-latency model, the free parameters are $(H_0, \Omega_{F0}, \beta_1, \Delta, \sigma_{8,0})$; for Λ CDM, the free parameters are $(H_0, \Omega_{m0}, \sigma_{8,0})$.

Table I summarizes the resulting best-fit points. The raw χ^2 values are nearly degenerate: the unconstrained v36.5 best fit reaches $\chi^2 = 29.49$, the finite-memory branch with $\Delta \geq 0.05$ gives $\chi^2 = 29.54$, and the best-fit Λ CDM comparison gives $\chi^2 = 29.56$. The important qualitative result is that the unconstrained fit drives the preferred region toward the Markovian edge, with $\Delta \simeq 2.4 \times 10^{-3}$. Even when a finite-memory prior is imposed, however, the fit remains almost indistinguish-

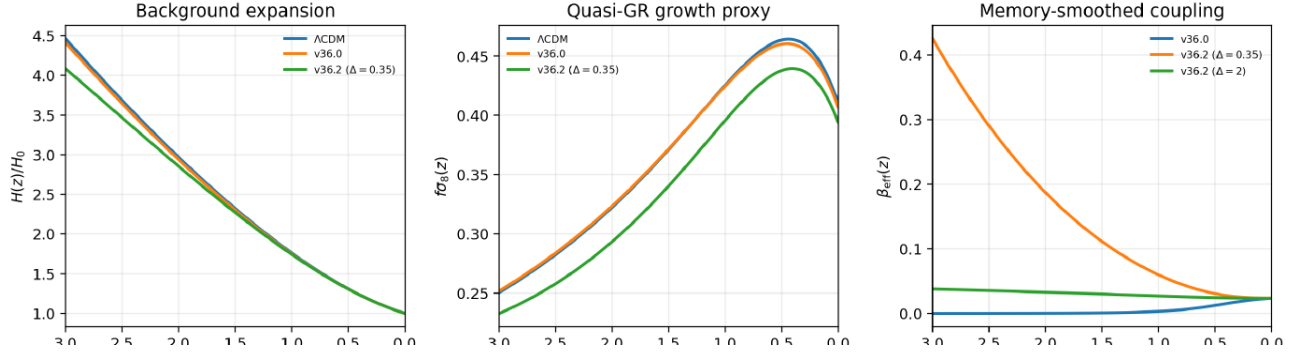


FIG. 1. Illustrative benchmark comparison inherited from MetaTime v36.2. Left: exact background expansion histories. Center: quasi-GR proxy for $f\sigma_8(z)$ computed on the same backgrounds. Right: memory-smoothing of the effective coupling, showing both the representative benchmark $\Delta = 0.35$ and a larger- Δ frozen-memory regime. Since v36.5 preserves the operational cosmological equations inherited from v36.4, these benchmark curves remain unchanged; what is new is the explicit derivational bridge linking them to future-latency closure and the additional expansion-growth hysteresis diagnostic.

able from Λ CDMin raw χ^2 . Information criteria continue to favor Λ CDM because the future-latency model carries more free parameters in this pilot setup.

Figure 4 shows the corresponding best-fit curves against the late-time data points. The left panel compares the expansion histories to the cosmic-chronometer compilation, while the right panel compares the quasi-GR growth proxy to the $f\sigma_8$ compilation. The pilot message is disciplined rather than triumphant: present late-time data do not require strong memory, but they also do not rule out the model's minimally non-Markovian regime. A full assessment of the hysteresis observable will ultimately require CLASS/CAMB-level transfer functions and a joint likelihood with realistic covariance structure.

XI. EXPANDED CERTIFICATION LOGIC

The v36.2 validation structure is retained with minimal modification:

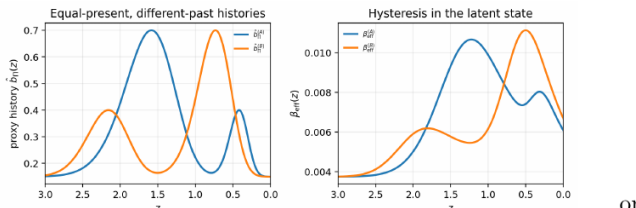


FIG. 2. Operational hysteresis benchmark inherited from MetaTime v36.2. Two proxy histories with equal present value but different past support generate distinct latent states and therefore distinct present effective couplings when $\Delta > 0$. In v36.5 the same effect is read as path dependence in the locally available future.

1. *Uncoupled regression*: $\beta_0 = \beta_1 = 0$ must recover Λ CDM.

2. *Bookkeeping conservation*: monitor

$$R(a) \equiv \frac{d\rho_{\text{tot}}}{d \ln a} + 3(\rho_{\text{tot}} + p_{\text{tot}}), \quad (35)$$

and require numerical consistency.

3. *Radiation-era safety*: enforce a conservative BBN prior $|Q|/(H\rho_{\text{tot}}) < \epsilon_{\text{BBN}}$ at high redshift.

4. *Super-Hubble boundedness*: verify stability of gauge-invariant curvature perturbations.

5. *Markovian regression*: $\Delta \rightarrow 0$ must collapse continuously to v36.0.

6. *Hysteresis test*: distinct proxy histories with identical present value must produce distinct present effective couplings whenever $\Delta > 0$.

7. *Controlled-proxy test*: the extended perturbation system with $b_{\Pi} \neq 0$ must reduce continuously to the minimal closure as $b_{\Pi} \rightarrow 0$.

These tests separate numerical stability, regression to the local limit, and the physical significance of the proxy-perturbation approximation. In v36.5 they also test the new interpretive bridge and its observable consequence: if the benchmark curves and hysteresis protocol survive full Boltzmann implementation and likelihood confrontation, the observationally relevant content is no longer merely that the coupling is non-local, but that the latent sector behaves as a history-bearing reservoir of future latency.

XII. CONCLUSIONS

MetaTime v36.5 preserves the core achievements of v36.2: a solver-ready non-Markovian dark-sector closure

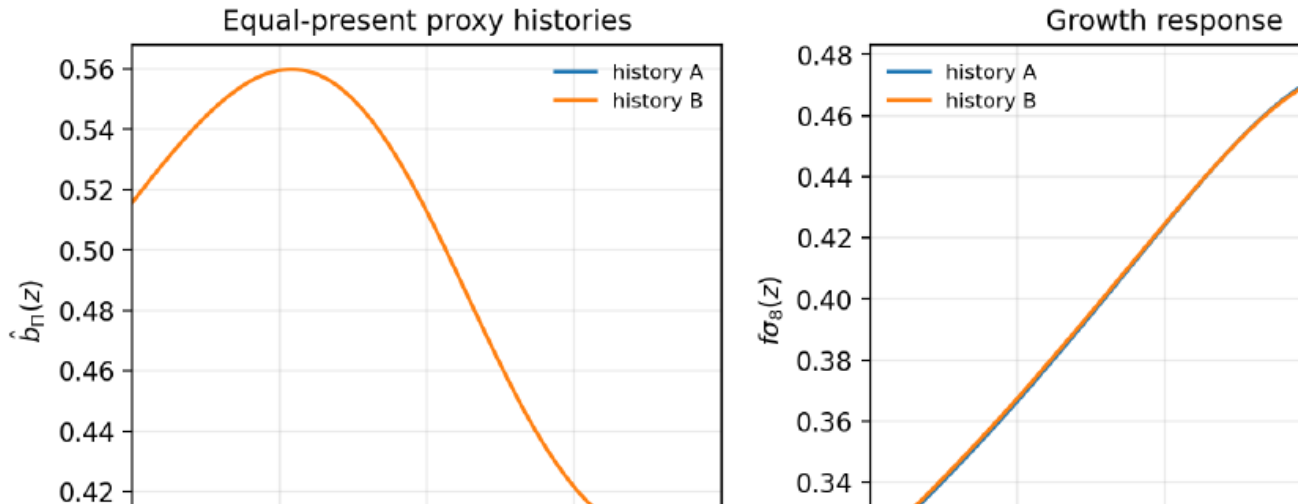


FIG. 3. New v36.5 toy benchmark illustrating expansion-growth hysteresis. Left: two proxy histories with equal present value but different past support. Center: the corresponding growth responses, plotted as $f\sigma_8(z)$. Right: the resulting finite band in the $(H/H_0, f\sigma_8)$ plane, quantified by the area functional $\mathcal{A}_{\text{hyst}}$ defined in Eq. (33). In the Markovian limit this area collapses to zero; for finite Δ it provides a direct observable summary of non-Markovian future-latency dynamics.

TABLE I. Pilot fit summary for the late-time comparison shown in Fig. 4. The v36.5 entries use the same benchmark proxy history as the main text and a quasi-GR growth proxy. This table is intended as a preliminary phenomenological check rather than a full cosmological likelihood analysis.

Model	H_0	Ω_{F0} or Ω_{m0}	β_1	Δ	$\sigma_{s,0}$	χ^2	AIC	BIC
v36.5 best fit	68.884	0.2599	0.03199	0.00238	0.8044	29.49	39.49	49.70
v36.5 best fit ($\Delta \geq 0.05$)	68.782	0.2572	0.01410	0.05003	0.8017	29.54	39.54	49.75
Λ CDM best fit	68.901	0.3028	—	—	0.8013	29.56	35.56	41.69

with a strict regression channel to v36.0, a physically anchored memory width, an open-EFT motivation for the retarded kernel, controlled perturbations, and benchmark observables. The technical implementation remains conservative by design.

The v36.4 step made the closure logic more explicit, and the new v36.5 step promotes that logic into a sharper observable. We identify the latent sector with future latency, $\rho_L \equiv \rho_F$, and show that once one treats that sector as a finite-bandwidth stock of physically weighted but not-yet-executed state capacity, a leading-order exchange law proportional to $H\rho_F$ is the natural effective choice. The v36.2 closure is therefore reinterpreted not as a free-floating ansatz, but as the minimal stock-flow law compatible with conservation, FRW scaling, delayed accessibility, and regression to the local limit.

This still does not constitute a unique UV derivation, nor does it replace the need for full CLASS/CAMB likelihood confrontation. But it does strengthen the scientific status of the framework in two distinct ways. First, the cosmological machinery and the MetaTime ontology are no longer merely adjacent; they are linked by an explicit

effective closure argument. Second, the model now comes with a sharper observational target: a finite hysteresis area in the $(H/H_0, f\sigma_8)$ plane at matched present proxy value. If future analyses show that observables such as $H(z)$, $f\sigma_8(z)$, or late-time gravitational potentials depend on past proxy support at fixed present value, then the model realizes a genuinely non-Markovian cosmology that may be read as a test of future-latency dynamics in the dark sector. In that sense, v36.5 does not only reinterpret delayed-response exchange; it proposes a concrete summary statistic for it. The pilot late-time comparison added here sharpens that conclusion. At the level of a simple diagonal-error test, the framework remains competitive with Λ CDM in raw χ^2 , but the preferred region lies close to the Markovian limit. That is a scientifically useful result in its own right: it means the model is not immediately ruled out by present $H(z) + f\sigma_8$ data, while also showing that a decisive test of genuinely finite memory will require stronger data combinations and a full Boltzmann-likelihood implementation.

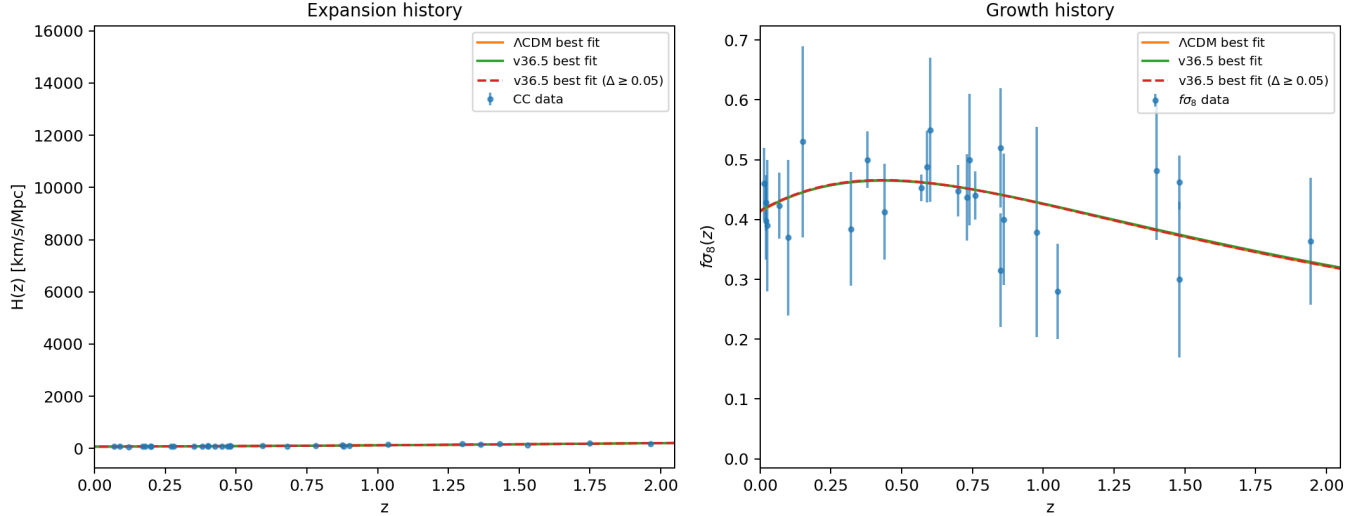


FIG. 4. Pilot comparison of v36.5 against public late-time data. Left: best-fit expansion histories plotted against the 31-point cosmic-chronometer compilation. Right: best-fit quasi-GR growth histories plotted against the 26-point $f\sigma_8$ compilation. The unconstrained best fit prefers a near-Markovian memory width, while the finite-memory branch with $\Delta \geq 0.05$ remains nearly degenerate with Λ CDM in raw χ^2 .

ACKNOWLEDGMENTS

The author thanks Stephen Atalebe for useful discussions that helped motivate the study of memory-bearing dark-sector closures. Any remaining shortcomings are the author's own.

Appendix A: Kernel-to-ODE equivalence

Starting from Eq. (7), differentiation with respect to x yields

$$m'(x) = \frac{\hat{b}_\Pi(x) - m(x)}{\Delta}, \quad (\text{A1})$$

which is Eq. (10). More general kernels may be represented by Prony-series embeddings with multiple auxiliary memory variables.

Appendix B: Operational hysteresis protocol

Choose two proxy histories,

$$\hat{b}_\Pi^{(A)}(x) = \hat{b}_{\Pi,0} + A \exp[-(x - x_*)^2/\sigma^2], \quad (\text{B1})$$

$$\hat{b}_\Pi^{(B)}(x) = \hat{b}_{\Pi,0} + A \exp[-(x - x_{**})^2/\sigma^2], \quad (\text{B2})$$

with $x_* \neq x_{**}$ but arranged so that $\hat{b}_\Pi^{(A)}(0) = \hat{b}_\Pi^{(B)}(0) = \hat{b}_{\Pi,0}$. For any $\Delta > 0$, the corresponding solutions of Eq. (10) generically satisfy $m^{(A)}(0) \neq m^{(B)}(0)$, while the difference collapses as $\Delta \rightarrow 0$.

-
- [1] D. Peyr , *MetaTime v36.1: Non-Markovian Cosmological Dynamics from Processing-Driven Dark-Sector Exchange*, unpublished manuscript (2026).
 - [2] D. Peyr , *MetaTime v36.2: Non-Markovian Cosmological Dynamics from Processing-Driven Dark-Sector Exchange: Physically Anchored Memory, Controlled Perturbations, and Illustrative Observable Benchmarks*, unpublished manuscript (2026).
 - [3] D. Peyr , *MetaTime XVIII: Dark Matter as Uncompressed Future Latency and the Caching Buffer of the Universe*, unpublished manuscript (2026).
 - [4] L. Amendola, Phys. Rev. D **62**, 043511 (2000).
 - [5] J. Valiviita, E. Majerotto, and R. Maartens, JCAP **07**, 020 (2008).
 - [6] C.-P. Ma and E. Bertschinger, Astrophys. J. **455**, 7 (1995).
 - [7] W. Hu and I. Sawicki, Phys. Rev. D **76**, 104043 (2007).
 - [8] W. Fang, W. Hu, and A. Lewis, Phys. Rev. D **78**, 087303 (2008).
 - [9] A. Lewis and S. Bridle, Phys. Rev. D **66**, 103511 (2002).
 - [10] A. Lewis, A. Challinor, and A. Lasenby, Astrophys. J. **538**, 473 (2000).
 - [11] R. P. Feynman and F. L. Vernon, Ann. Phys. **24**, 118 (1963).
 - [12] J. S. Schwinger, J. Math. Phys. **2**, 407 (1961).
 - [13] L. V. Keldysh, Sov. Phys. JETP **20**, 1018 (1965).